

Multinucleon transfer reactions for the $^{28}\text{Si}+^{90,94}\text{Zr}$ systems in the region below and near the Coulomb barrier

Sunil Kalkal,^{1,*} S. Mandal,¹ N. Madhavan,² A. Jhingan,² E. Prasad,³ Rohit Sandal,⁴ S. Nath,² J. Gehlot,² Ritika Garg,¹ Gayatri Mohanto,² Mansi Saxena,¹ Savi Goyal,¹ S. Verma,¹ B. R. Behera,⁴ Suresh Kumar,¹ U. D. Pramanik,⁵ A. K. Sinha,⁶ and R. Singh^{1,†}

¹*Department of Physics & Astrophysics, University of Delhi, Delhi, India*

²*Inter University Accelerator Centre, New Delhi, India*

³*Department of Physics, Calicut University, Kerala, India*

⁴*Department of Physics, Panjab University, Chandigarh, India*

⁵*Saha Institute of Nuclear Physics, Kolkata, India*

⁶*UGC-DAE Consortium for Scientific Research, Kolkata, India*

(Received 13 January 2011; revised manuscript received 3 March 2011; published 17 May 2011)

Measurements on multinucleon transfer reactions for $^{28}\text{Si} + ^{90,94}\text{Zr}$ systems were performed at sub- and near-barrier energies. The fact that ^{90}Zr has a closed neutron shell ($N = 50$) and ^{94}Zr has four neutrons outside the closed shell, allows us to investigate the effects of shell closure and pairing correlation on multinucleon transfer mechanism. The experiment was performed with pulsed ^{28}Si beam using the Heavy Ion Reaction Analyzer (HIRA) at Inter University Accelerator Centre (IUAC), New Delhi. Based on the Q -value considerations, it turned out that pickup channels were neutron transfer whereas stripping channels were proton transfer. For the $^{28}\text{Si} + ^{90}\text{Zr}$ system, the values of the slope parameter for two-neutron pickup turned out to be less than that for one-neutron pickup. The values of the slope parameter were almost the same for two-, three-, and four-neutron pickup channels in the case of the $^{28}\text{Si} + ^{94}\text{Zr}$ system. The transfer probabilities in the case of the $^{28}\text{Si} + ^{94}\text{Zr}$ system were much larger than those for the $^{28}\text{Si} + ^{90}\text{Zr}$ system, further supporting the fact that there is a correlation between the transfer channels and sub-barrier fusion cross-section enhancement. An odd-even staggering was observed in the extracted transfer probabilities at the barrier radius implying the role of pairing correlation in transfer reactions.

DOI: [10.1103/PhysRevC.83.054607](https://doi.org/10.1103/PhysRevC.83.054607)

PACS number(s): 25.70.Hi

I. INTRODUCTION

Heavy-ion collisions around the Coulomb barrier offer a very rich variety of phenomena and their coupling effects on each other [1,2]. It is in this energy regime where transfer reactions constitute a significant part of the reaction cross section. The transfer reactions serve a wide range of objectives like estimation of relative and absolute spectroscopic factors of nuclear levels [3], understanding the correlations between nucleons [4], and the transition from the quasielastic to deep inelastic regime [1], etc. These reactions can also be used to populate moderately high spin states of nuclei [5–7] for spectroscopic studies. The multinucleon transfer reactions are a very useful tool to study exotic nuclei [8,9]. Multinucleon transfer can take place either simultaneously or sequentially, indicating interplay of the nuclear reactions and structure. However, the mechanism and many other features of multinucleon transfer reactions are still not very well understood [3,4,10,11]. Multinucleon transfer is a multistep process in which the colliding nuclei can be inelastically excited before or after the transfer. The number of such possibilities increases drastically with an increasing number of transferred nucleons, and it becomes very tedious to ascertain the reaction mechanism.

In the sub-barrier region, little data exist on multinucleon transfer reactions because of various kinds of technical difficulties involved in these measurements [12–18]. The transfer cross sections are very low at the sub-barrier energies, and there are rather high elastic cross sections in this energy region. The reaction products in these reactions are backward peaked (180°) in the center-of-mass system and forward-moving recoils are peaked around 0° . Moreover, the energies of forward-moving recoils, as well as those of the back-scattered particles, are less than 1 MeV/nucleon, rendering the particle identification extremely difficult. Thus, a recoil mass spectrometer turns out to be a very efficient device for such measurements.

Here we report the results of the measurements on the multinucleon transfer for $^{28}\text{Si} + ^{90,94}\text{Zr}$ systems at sub- and near-barrier energies. The measurements were performed in the sub-barrier region for the study of nuclear correlations near the ground state. As ^{90}Zr has a closed neutron shell ($N = 50$), the effect of shell closure on neutron transfer can be studied. On the other hand, ^{94}Zr has four neutrons outside the closed shell, therefore, one can investigate the effects of pairing correlation on multinucleon transfer reactions. The enhancement observed in the transfer probability for the transfer of an even number of nucleons was very controversial. The enhancement in an even number of neutron transfers is observed in some cases [19–21] and not in others [22–24]. In the cases where enhancement was not observed, it was found

*kalkal84@gmail.com

†Present address: AINST, Amity University, NOIDA (UP).

that for each successive neutron transfer the cross section was falling by a factor of 3–5 and no enhancement was observed in the cross sections for $2n$, $4n$, $6n$ transfer with respect to $1n$, $3n$, $5n$ transfer. The enhancement for an even number of proton transfers was also observed in a few cases [25–27].

II. EXPERIMENTAL DETAILS

The experiment was performed with a pulsed ^{28}Si beam having a pulse separation of $1\ \mu\text{s}$ (1.5-ns width) using HIRA [28] at IUAC, New Delhi. The targets used were isotopically enriched $^{90,94}\text{Zr}$ (97.65% and 96.07%, respectively) $280\text{-}\mu\text{g}/\text{cm}^2$ thick foils prepared on $45\text{-}\mu\text{g}/\text{cm}^2$ carbon backings [29]. In the target chamber of HIRA, two silicon surface barrier detectors were placed at $\pm 25^\circ$ to monitor the beam. To improve the beam rejection, HIRA was rotated to 6° . A silicon surface barrier detector (SSBD) of a $20 \times 20\ \text{mm}^2$ active area was placed at a back angle to set up kinematic coincidence between forward-moving targetlike recoiling particles and back-scattered projectilelike nuclei. The angular position of SSBD was optimized by maximizing the coincidence counts between this detector and the focal plane detector. This resulted in the final angular position of the SSBD at 166° with which the data were taken. A carbon charge reset foil of $35\text{-}\mu\text{g}/\text{cm}^2$ thickness was used for charge equilibration of recoiling particles produced during the reaction. At the focal plane of HIRA, a multiwire proportional counter (MWPC) of a $150 \times 50\ \text{mm}^2$ active area was used for the detection of recoiling particles. The time-of-flight spectrum (MWPC-RF-TAC) was obtained with the arrival of particles at the focal plane MWPC as the start and RF of the beam as the stop signal to separate the multiply scattered beamlike and recoiling targetlike particles at the focal plane. Another time of flight (MWPC-SSBD-TAC) was defined by taking the MWPC anode signal as the start and delayed back-angle SSBD signal as the stop. This was helpful in removing the beamlike background. The measurements were performed at beam energies of 83.3, 86.4, 89.5, 92.5, and 95.5 MeV in the laboratory frame (after taking beam energy losses in the targets into account). The nominal lab Coulomb barriers for $^{28}\text{Si} + ^{90,94}\text{Zr}$ systems are 95.8 and 94.2 MeV, respectively. The solid angle of acceptance for HIRA was kept 5 msr ($6^\circ \pm 2.28^\circ$) for carrying out these measurements. A gated (by MWPC-RF-TAC and MWPC-SSBD-TAC) correlation spectrum between MWPC-RF-TAC and MWPC positions for $^{28}\text{Si} + ^{94}\text{Zr}$ at 92.5 MeV is shown in Fig. 1. From the Q -value considerations, it was found that pickup channels were neutron transfer whereas stripping channels were proton transfer. A list of the ground-state Q values for various transfer channels for both the systems is given in Table I. As the neutron transfer channels have positive Q values (Table I), the kinetic energies of the recoiling particles for these channels are more than those of the elastic recoils. In addition, the masses of the recoiling particles decrease with the increase in the number of neutrons transferred. Consequently, the time of flight of the recoils reduces with a decrease in the mass. As mentioned earlier, the MWPC-RF-TAC was defined taking RF as stop, and the resulting output is presented on the ordinate in Fig. 1. Along the ordinate, the time of flight

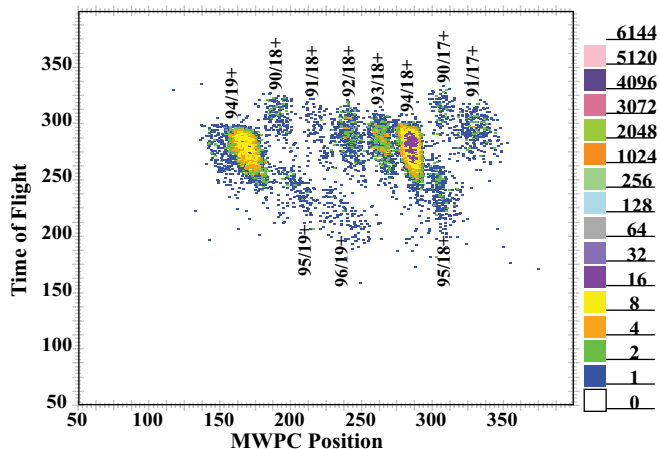


FIG. 1. (Color online) A correlation spectrum between time of flight and MWPC position of recoiling particles for $^{28}\text{Si} + ^{94}\text{Zr}$ at 92.5 MeV.

decreases with an increase in the channel number. Thus, the higher the channel number is along the ordinate, the lesser the value of the actual time of flight. On the other hand, the proton transfer channel that leads to recoiling the ^{95}Nb nucleus, has a negative Q value (Table I). These recoiling particles are heavier than the elastic recoil and have less energy (hence, less velocity). Thus, these particles have longer time of flight and the structure labeled $95/18^+$ is significantly lower than the other masses with $q = 18^+$ along the ordinate. A gated (by MWPC-RF-TAC and MWPC-SSBD-TAC) one-dimensional projected mass spectrum of recoiling targetlike particles for $^{28}\text{Si} + ^{94}\text{Zr}$ at 95.5 MeV is shown in Fig. 2. The transfer channels up to four-neutron pickup and one-proton stripping can be noted in Figs. 1 and 2. We could clearly resolve m/q ambiguity [very close m/q values for $95/18^+$ (proton stripping) and $90/17^+$ (four-neutron pickup) can only be resolved perhaps by using time-of-flight technique in such an experimental setup) by the time of flight technique (see Fig. 1). An extreme low-energy run was taken at 70 MeV (much below the Coulomb barrier so that the transfer probability is negligibly small) to determine the isotopic contents of the targets experimentally. The extracted values for isotopic contents were found to be consistent with the values provided by the supplier. The energy (E), charge state (q), and mass (m) of the recoils were scanned in an iterative way to maximize the HIRA transmission efficiency for the recoiling particles reaching the focal plane.

TABLE I. Ground-state Q values for various transfer channels for $^{28}\text{Si} + ^{90,94}\text{Zr}$ systems.

System	Channel	$Q_{g.s.}$ (MeV)	Channel	$Q_{g.s.}$ (MeV)
$^{28}\text{Si} + ^{94}\text{Zr}$	+1n	0.252	-1p	-4.781
	+2n	4.127	-1n	-10.718
	+3n	2.080	+4n	4.088
$^{28}\text{Si} + ^{90}\text{Zr}$	+1n	-3.496	+3n	-7.963
	+2n	-2.204		

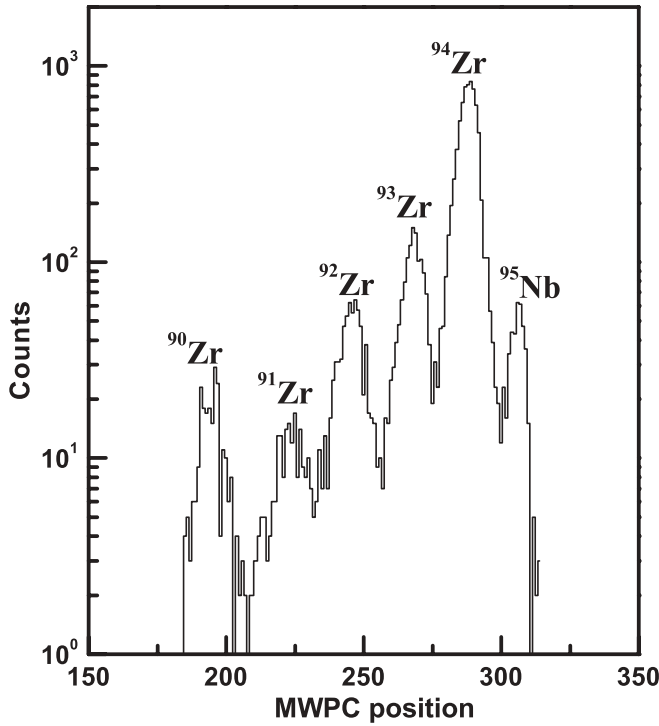


FIG. 2. The mass spectrum obtained by projecting the correlation spectrum between time of flight and MWPC position on the x axis for $^{28}\text{Si} + ^{94}\text{Zr}$ at 95.5 MeV.

III. RESULTS AND DISCUSSION

Transfer products along with the elastic recoils were focused according to their m/q values at the focal plane of HIRA. As the solid angle factor (the fraction of transfer channels accepted by the solid angle acceptance of the spectrometer) is independent of the transfer reaction channels, the yields of these channels can be used directly for extracting the transfer probabilities. The transfer probability was taken as the ratio of the yield of the particular transfer channel (Y_{tr}) to the total yield of elastic, inelastic, and transfer channels (quasielastic yield dominated by elastic channel) (Y_{qe}), that is,

$$P_{tr} = \frac{Y_{tr}}{Y_{qe}} \times \eta_m.$$

The mass correction factor, η_m , (position-dependent efficiency factor) was taken into account while extracting the transfer probabilities. The position-dependent efficiency factor was extracted by moving the elastic recoils across the focal plane of the HIRA by varying the HIRA settings (changing the mass of recoiling particles). The ratio of the yield of elastic to the geometric mean of the monitors was plotted against the MWPC position to extract the position-dependent efficiency factor. The transfer probabilities for one- and two-neutron pickup channels for ^{94}Zr turned out to be much more than those for ^{90}Zr . The sub-barrier fusion cross sections were found to be much more enhanced in the case of $^{28}\text{Si} + ^{94}\text{Zr}$ as compared to $^{28}\text{Si} + ^{90}\text{Zr}$ [30], suggesting a correlation between the transfer reactions and sub-barrier fusion cross-section enhancement, as observed by L. Corradi *et al.* [31] also. The

transfer of neutrons initiates the fusion at the large distances as there is no Coulomb barrier involved and hence leads to sub-barrier fusion cross-section enhancement. The major transfer channels observed for the ^{94}Zr target were up to four-neutron pickup and one-proton stripping, whereas in the case of ^{90}Zr , only up to two-neutron pickup channels were observed. The fewer number of neutron transfer channels with small values of transfer probabilities for the ^{90}Zr target could be associated with the neutron shell closure. For heavy ions in the near-barrier regions (Sommerfeld parameter, $\eta \gg 1$), a semiclassical formalism [3,4] of scattering can be applied. It can be assumed that the incident particle follows the Coulomb trajectory and the transfer probability is maximum at the distance of closest approach (i.e., the turning point) between the colliding ions. The distance of the closest approach (D_0) is defined as (assuming pure Coulomb trajectory)

$$D_0 = \frac{Z_P Z_T e^2}{2E_{c.m.}} (1 + \cos \theta_{c.m.}) = d_0 (A_P^{1/3} + A_T^{1/3}).$$

Here, $E_{c.m.}$ and $\theta_{c.m.}$ are the energy of the incident particles and angle of the projectilelike particles in the center-of-mass system, respectively, and d_0 is the distance parameter. A_P (Z_P) and A_T (Z_T) are the projectile and target mass numbers (atomic numbers), respectively. In the energy region where the present measurements were performed (i.e., $d_0 \geq 1.5$ fm), the effect of nuclear interactions can be neglected [3]. In Figs. 3 and 4 the extracted transfer probabilities versus the distance

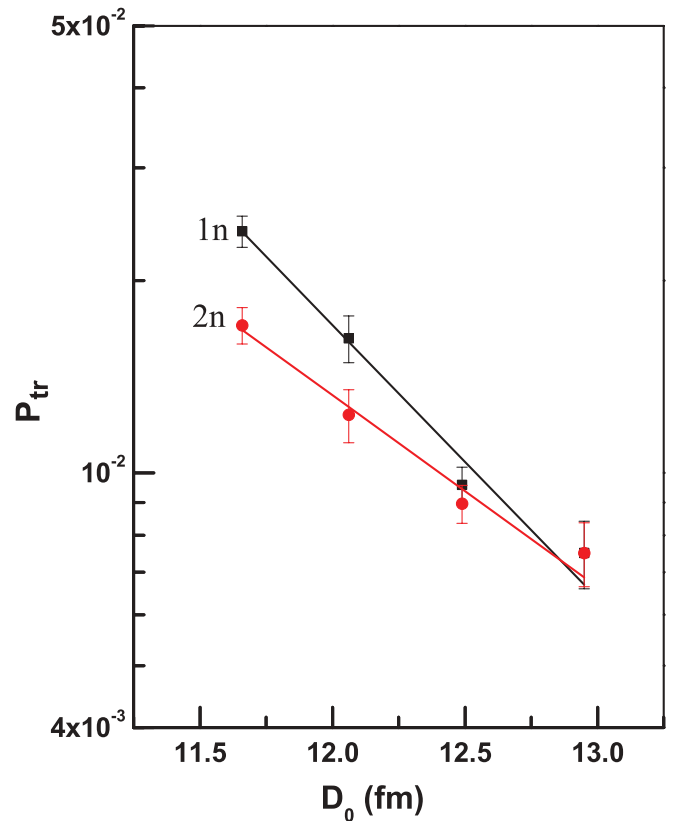


FIG. 3. (Color online) Transfer probability (P_{tr}) versus distance of closest approach (D_0) plot for $^{28}\text{Si} + ^{90}\text{Zr}$ (see the text). The straight lines are the best fits through the data points.

of closest approach are plotted for the $^{28}\text{Si} + ^{90,94}\text{Zr}$ systems, respectively. The errors shown in the figures are the statistical errors. Because the transfer reactions in the sub-barrier region take place via tunneling of nucleons through the barrier between the colliding nuclei, the exponential dependence of the transfer probabilities on the distance of closest approach can be assumed. The probability data were fitted to obtain $P_{tr}(R_B)$ [the transfer probability at the barrier radius, given by $R_B = 1.4(A_P^{1/3} + A_T^{1/3})$] and the experimental slope parameter (α_{expt}) using the expression,

$$P_{tr}(D_0) = P_{tr}(R_B) \exp[-2\alpha_{\text{expt}}(D_0 - R_B)].$$

Theoretical slope parameter (α_{th}) was taken as the average of the slope parameters for the donor (i) and acceptor nuclei (f) and was defined as

$$\alpha_{\text{th}} = \frac{1}{2}(\alpha_i + \alpha_f); \quad \text{with} \quad \alpha_k = \sqrt{\frac{2\mu_k[(E_B)_{\text{eff}}]_k}{\hbar^2}},$$

where μ is the reduced mass of the donor or acceptor nucleus and $(E_B)_{\text{eff}}$ is the effective binding energy of the transferred nucleons. The effective binding energy for the transferred neutron is the same as the usual binding energy, (E_B^0) , as these particles do not experience any Coulomb force, but for the transferred proton the effective binding energy was taken as [32]

$$(E_B)_{\text{eff}} = E_B^0 - \Delta V + V_C,$$

where ΔV is the change in the binding energy because of the Coulomb field of the approaching collision partner and V_C is the Coulomb barrier that the transferred proton has to overcome. If Z_C is the number of the transferred protons, Z_P the atomic number of the approaching collision partner, and R_C the Coulomb radius then the ΔV can be calculated using $\Delta V = Z_C Z_P e^2 / R_C$.

The values of the experimentally obtained slope parameters along with the theoretically calculated ones have been listed in Table II. From this table, it may be noted that for the $^{28}\text{Si} + ^{94}\text{Zr}$ system the experimental and theoretical values of the slope parameter for one-proton transfer channel agree reasonably well. However, for the neutron transfer channels, the experimental values of the slope parameters are generally significantly lower than the theoretical values for both the systems. The transfer probabilities at the barrier radius, obtained by fitting transfer probability versus distance of closest approach (D_0) data, are also listed in Table II. It was found that for both the systems, the transfer probability at the barrier radius for two-neutron pickup is almost half of that for the one-neutron pickup. For the $^{28}\text{Si} + ^{94}\text{Zr}$ system, the transfer probability for three-neutron pickup is a factor of 5 smaller than that for two-neutron pickup and the transfer probability for four-neutron pickup was found to be almost the same as that for three-neutron pickup. Thus, some kind of odd-even staggering for neutron transfer channels is observed in these systems which could be from pairing correlations as shown in Fig. 5 (for the $^{28}\text{Si} + ^{94}\text{Zr}$ system). In this figure, it can be noted that there is some enhancement observed in the transfer probabilities at the barrier radius (indicated by arrows) in

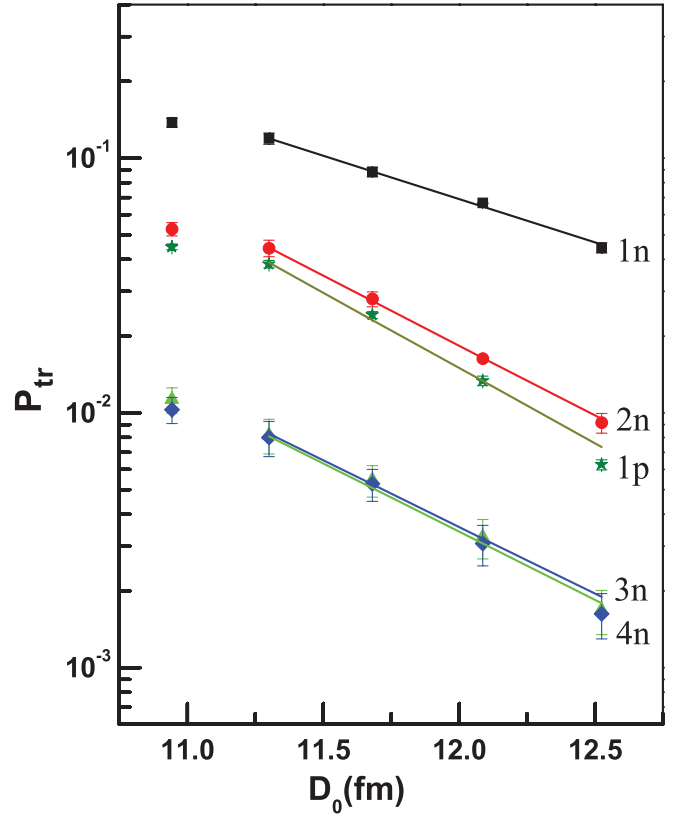


FIG. 4. (Color online) Transfer probability (P_{tr}) versus distance of closest approach (D_0) plot for $^{28}\text{Si} + ^{94}\text{Zr}$ (see the text). The straight lines are the best fits through the data points.

two- and four-neutron transfer channels. If two- and four-neutron transfer probabilities also happen to lie on the same line as the ones for one- and three-neutron transfer channels, then a reduction in the transfer probability by an approximately constant factor of 3 would be observed for each transferred neutron. This is suggestive of significant contributions from the simultaneous transfer in addition to sequential transfer for multinucleon transfer reactions. It was further noted that the transfer probability for one-neutron pickup for the $^{28}\text{Si} + ^{94}\text{Zr}$ system was a factor of two higher as compared to the one-proton stripping which could be attributed to the subshell closure for protons. For the $^{28}\text{Si} + ^{94}\text{Zr}$ system, the experimental slope parameter remains constant beyond two-neutron pickup. A similar behavior was observed in the case of the $^{58}\text{Ni} + ^{124}\text{Sn}$ [17] system where the slope parameter remained constant from three-neutron pickup to six-neutron pickup channels.

In Table II, the values of the transfer form factors extracted from the data at the barrier radius are also given. For the extraction of the transfer form factor, the first-order perturbation approximation was used. In this approximation, for a transfer channel β (corresponding to a particular state of the final nucleus) with Q_β as the transfer Q value, the transfer probability is related to the transfer form factor $F_\beta(R_B, Q_\beta)$ as [33]

$$P_{tr}(R_B, Q_\beta) = \frac{\pi}{\sigma^2} |F_\beta(R_B, Q_\beta)|^2 \exp\left[-\frac{(Q_\beta - Q_{\text{opt}})^2}{2\sigma^2}\right],$$

TABLE II. Transfer probabilities at the barrier radius (R_B), experimentally extracted (α_{expt}) and theoretically calculated slope parameters (α_{th}), and the form factors for the $^{28}\text{Si} + ^{90,94}\text{Zr}$ systems for various channels.

System	Channel	$P_{\text{tr}}(R_B)$	α_{th}	α_{expt}	F_0
$^{28}\text{Si} + ^{94}\text{Zr}$	+1n	0.2037 ± 0.0061	0.6247	0.3908 ± 0.0141	0.2732
	+2n	0.1053 ± 0.0026	1.2449	0.6317 ± 0.0135	0.1679
	+3n	0.0188 ± 0.0012	1.8174	0.6014 ± 0.0346	0.0752
	+4n	0.0188 ± 0.0011	2.3958	0.6163 ± 0.0303	0.0705
$^{28}\text{Si} + ^{90}\text{Zr}$	-1p	0.0984 ± 0.0073	0.6853	0.6801 ± 0.0409	0.3078
	+1n	0.0728 ± 0.0084	0.6891	0.4922 ± 0.0401	0.7798
	+2n	0.0367 ± 0.0037	1.3581	0.3453 ± 0.0331	0.3086

where Q_{opt} is the optimum Q value for the transfer to take place and σ is the width of the Q -value distribution (the standard deviation). Here σ and Q_{opt} are given by

$$\sigma = \sqrt{\frac{\alpha \hbar^2 \ddot{r}}{2}}; \quad \ddot{r} = \frac{2E_{\text{c.m.}} - E_B}{m_a A R_B}$$

$$Q_{\text{opt}} = \left(\frac{Z_p^f Z_T^f}{Z_p^i Z_T^i} - 1 \right) E_{\text{c.m.}}$$

In the above expressions, $E_{\text{c.m.}}$ is the energy in the center-of-mass system, α the slope parameter obtained experimentally, \ddot{r} the acceleration at the turning point, $m_a A$ the reduced mass of the incident channel, E_B the barrier height, and R_B the barrier radius. In the expression for Q_{opt} , f is used for the final channel and i for the initial channel, and Z_p and Z_T are the atomic numbers of projectile and target, respectively. The Q_{opt} is zero for neutron transfer channels. As the resolution of the detector was not good enough to resolve states of the detected nuclei and, therefore, if the transfer probability is integrated over the Q value then the expression for transfer

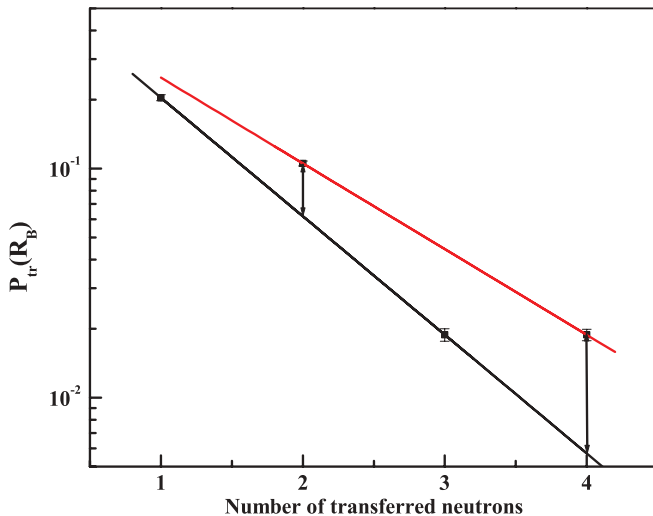


FIG. 5. (Color online) Transfer probability at the barrier radius [$P_{\text{tr}}(R_B)$] versus neutron numbers transferred plot for the $^{28}\text{Si} + ^{94}\text{Zr}$ system. The black (red) straight line is the best fit through the data for odd (even) number of nucleons transferred.

probability becomes [34]

$$P_{\text{tr}}(R_B) = \frac{\pi}{\sigma^2} \frac{d|F_B(R_B)|^2}{dQ} \int_{-\infty}^{Q_{\text{gs}}} \exp\left[-\frac{(Q - Q_{\text{opt}})^2}{2\sigma^2}\right] dQ.$$

Thus, a Q -value independent form factor is obtained. From the above expression, one can obtain the value of F_0 , which is defined as $F_0 = \sqrt{d|F_B(R_B)|^2/dQ}$. The values of the form factors so obtained are listed in Table II. It can be noted that the behavior of the transfer probabilities for various channels for both the systems gets reflected in the values of the form factors obtained from the data, as expected. These experimental values of the transfer form factors can be used as input to the detailed coupled channel calculations for explaining the role of transfer channels in the sub-barrier fusion cross-section

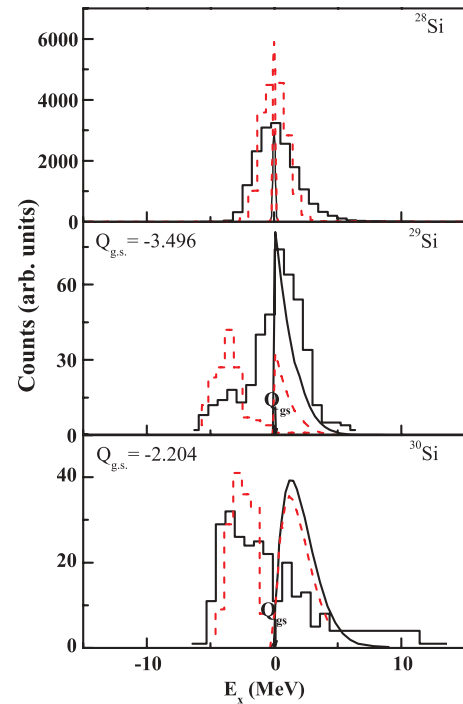


FIG. 6. (Color online) Excitation energy distributions of projectilelike particles for $^{28}\text{Si} + ^{90}\text{Zr}$ at 83.3 and 95.5 MeV. The dashed line is for 83.3 MeV and the solid line for 95.5 MeV. The step functions show the experimental distributions whereas the smooth lines depict the corresponding GRAZING calculations.

enhancement. Such a theoretical investigation would lead to a better understanding of the heavy-ion fusion at sub-barrier energies.

Figures 6 and 7 show the excitation energy spectra for both the systems at the lowest and the highest energies at which the data were taken (83.3 and 95.5 MeV, respectively). The excitation energy spectra were obtained from the back-angle SSBD. The energy spectrum from this detector was gated by the corresponding recoiling particles and was calibrated with respect to the elastically scattered ^{28}Si . From the expected energy values of the scattered projectilelike particles (obtained from the kinematics) and the obtained experimental energy spectra, the excitation energy spectra were obtained. In these figures, the step lines show the obtained experimental excitation energy spectra whereas the smooth lines show the excitation energy spectra obtained by using the code GRAZING [35]. The dashed lines are for 83.3 MeV and the solid lines are for 95.5 MeV. GRAZING is based on semiclassical theory [36] and it gives the capture and transfer cross sections along with the excitation energy distributions of transfer channels after the collision. This code includes independent

single-particle transfer for multinucleon transfer reactions and also the inelastic excitation to the low-lying states. The effects of neutron evaporation from the primary fragments were also taken into account.

For the $^{28}\text{Si} + ^{90}\text{Zr}$ system, the theoretical predictions agree quite well with the one-neutron transfer data but start deviating from the two-neutron transfer data as can be seen in Fig. 6. However, at 83.3 MeV, even for one-neutron pickup channel theoretical and experimental spectra do not agree, which could be because of the negative ground-state Q value. The excitation energy spectrum for $^{28}\text{Si} + ^{90}\text{Zr}$ is narrower at 83.3 MeV as compared to the one at 95.5 MeV. From Fig. 7, it is clear that for the $^{28}\text{Si} + ^{94}\text{Zr}$ system, the experimental and the theoretical excitation energy spectra match very well for one- and two-nucleon transfer reactions ($1n$ and $2n$ pickup and $1p$ stripping) at 95.5 MeV. However, at 83.3 MeV, the theoretical two-neutron pickup excitation energy distribution deviates slightly from experimentally obtained spectrum. At this energy, GRAZING predicts the higher excitation energy spectrum as compared to the experimental data. For three- and four-neutron pickup channels, there is some disagreement

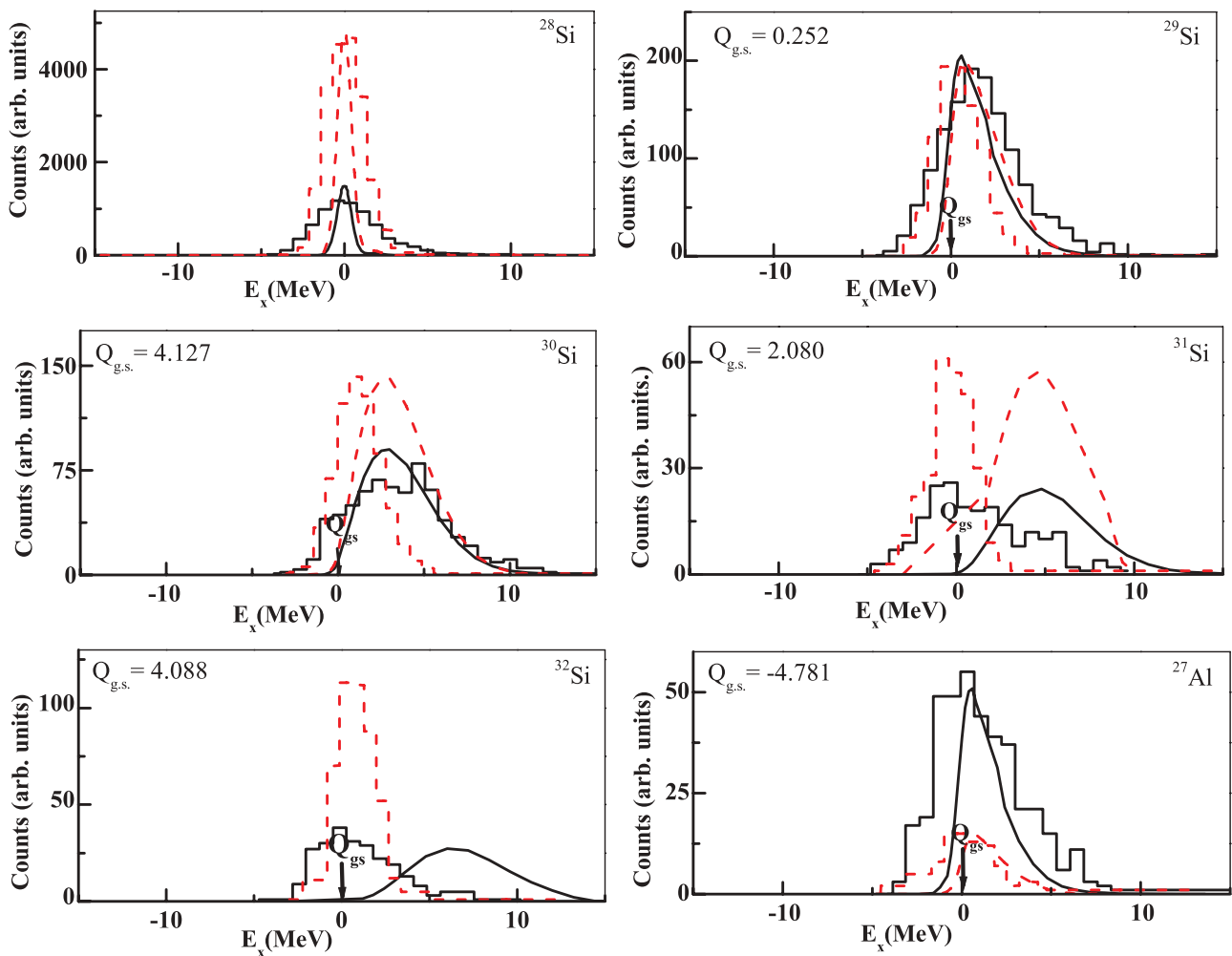


FIG. 7. (Color online) Excitation energy distributions of projectilelike particles for $^{28}\text{Si} + ^{94}\text{Zr}$ at 83.3 and 95.5 MeV. The dashed line is for 83.3 MeV and the solid line for 95.5 MeV. The step functions show the experimental distributions whereas the smooth lines depict the corresponding GRAZING calculations.

between the theoretical and the experimental spectra at both the energies. For three-neutron pickup, the theoretical predictions for the excitation energy are higher than the experimental values, and for four-neutron transfer the deviation is even more. Similar behavior was observed for theoretical predictions for multineutron transfer channels up to four-neutron pickup for the $^{58}\text{Ni} + ^{208}\text{Pb}$ system using the code GRAZING, but the calculations using Complex WKB [37] could reproduce the total kinetic energy loss spectrum reasonably well [38]. GRAZING does not make any prediction for the four-neutron pickup channel at sub-barrier energies, which was observed experimentally. It seems that the transfer is taking place from the ground state to the ground state and hence results in peaking at zero excitation energy. However, at 95.5 MeV, the excitation energy spectra are peaking at slightly higher excitation energies for one- and two-neutron pickup which may be from the excited state transfer. At 83.3 MeV, one-neutron transfer peaks at zero excitation energy. Here, it is to be mentioned once again that GRAZING doesn't include simultaneous transfer which may be an important mechanism of multinucleon transfer process at sub-barrier energies, and that may be the reason for the observed deviation for multineutron transfer in the present measurements. The excitation energy spectra at 95.5 MeV are broader as compared to the ones at 83.3 MeV, which may be considered as a clear evidence for cold transfer (from ground state to ground state) being the important mechanism for transfer at sub-barrier energies. No specific broadening of the excitation energy spectra for the multineutron transfer is observed in both the systems, giving a clear indication that in the sub-barrier region the transfer occurs mainly from ground state to ground state. Thus, no specific broadening of the spectra was observed with increase in the number of transferred nucleons.

IV. SUMMARY AND CONCLUSIONS

The results of multineutron transfer reaction studies for $^{28}\text{Si} + ^{90,94}\text{Zr}$ systems have been reported. For the $^{28}\text{Si} + ^{94}\text{Zr}$ system, up to four-neutron pickup and one-proton stripping channels were observed. From the Q-value considerations, it turned out that the nucleon pickup channels were neutron transfer and the stripping channels were proton transfer. It was also observed that the excitation energy spectra become broader with the increase in beam energy, which may be because of the excited state transfer taking place at higher energies. From the present results, it can be concluded that the simultaneous transfer is also an important mechanism of multineutron transfer reactions at the sub-barrier energies which may be from pairing correlations being stronger in the ground-state transfer. Another evidence of pairing correlation is the odd-even staggering of multineutron transfer probabilities at the barrier radius. The sub-barrier fusion cross sections [30] and the transfer probabilities are much higher for the $^{28}\text{Si} + ^{94}\text{Zr}$ system as compared to the $^{28}\text{Si} + ^{90}\text{Zr}$ system, providing evidence for correlation between the transfer and the fusion reactions.

ACKNOWLEDGMENTS

We are thankful to the Pelletron staff of the IUAC for providing a stable beam. We are grateful to the target laboratory staff, especially S. R. Abhilash, for helping in preparation of good-quality isotopic targets. Sunil Kalkal gratefully acknowledges CSIR, New Delhi for support. We acknowledge the help received from T. Varughese and S. Muralithar during these measurements. We express our gratitude to R. K. Bhowmik for many stimulating discussions. Two of the authors (M.S. and S.M.) acknowledge support from DAAD-DST.

-
- [1] K. E. Rehm, *Annu. Rev. Nucl. Part. Sci.* **41**, 429 (1991).
 [2] W. Reisdorf, *J. Phys. G* **20**, 1297 (1994).
 [3] C. Y. Wu, W. von Oertzen, D. Cline, M. W. Guidry, *Annu. Rev. Nucl. Part. Sci.* **40**, 285 (1990).
 [4] W. von Oertzen and A. Vitturi, *Rep. Prog. Phys.* **64**, 1247 (2001).
 [5] A. N. Wilson, C. W. Beausang, N. Amzal, D. E. Appelbe, S. Asztalos, P. A. Butler, R. M. Clark, P. Fallon, and A. O. Macchiavelli, *Eur. Phys. J. A* **9**, 183 (2000).
 [6] C. Wheldon *et al.*, *Eur. Phys. J. A* **20**, 365 (2004).
 [7] M. W. Guidry *et al.*, *Phys. Lett. B* **163**, 79 (1985).
 [8] H. Lenske and G. Schrieder, *Eur. Phys. J. A* **2**, 41 (1998).
 [9] Yu. E. Penionzhkevich, G. G. Adamian, and N. V. Antonenko, *Phys. Lett. B* **621**, 119 (2005).
 [10] W. R. Phillips, *Rep. Prog. Phys.* **40**, 345 (1977).
 [11] L. Corradi, G. Pollarolo, and S. Szilner, *J. Phys. G* **36**, 113101 (2009).
 [12] C. N. Pass *et al.*, *Nucl. Phys. A* **499**, 173 (1989).
 [13] K. E. Rehm, C. L. Jiang, J. Gehring, B. Glagola, W. Kutschera, M. D. Rhein, and A. H. Wuosmaa, *Nucl. Phys. A* **583**, 421 (1995).
 [14] R. R. Betts *et al.*, *Phys. Rev. Lett.* **59**, 978 (1987).
 [15] L. Corradi, A. M. Stefanini, D. Ackerman, S. Beghini, G. Montagnoli, C. Petrache, F. Scarlassara, C. H. Dasso, G. Pollarolo, and A. Winther, *Phys. Rev. C* **49**, R2875 (1994).
 [16] M. Devlin, D. Cline, R. Ibbotson, M. W. Simon, and C. Y. Wu, *Phys. Rev. C* **53**, 2900 (1996).
 [17] C. L. Jiang, K. E. Rehm, H. Esbensen, D. J. Blumenthal, B. Crowell, J. Gehring, B. Glagola, J. P. Schiffer, and A. H. Wuosmaa, *Phys. Rev. C* **57**, 2393 (1998).
 [18] D. O. Kataria *et al.*, *Phys. Rev. C* **56**, 1902 (1997).
 [19] I. Peter *et al.*, *Eur. Phys. J. A* **4**, 313 (1999).
 [20] W. Duennweber, H. Morinaga, and D. E. Alburger, *Phys. Lett. B* **106**, 47 (1981).
 [21] W. von Oertzen, H. G. Bohlen, B. Gebauer, R. Kunkel, F. Puhlhofer, and D. Schull, *Z. Phys. A* **326**, 463 (1987).
 [22] G. Montagnoli, S. Beghini, F. Scarlassara, G. F. Segato, L. Corradi, C. J. Lin, and A. M. Stefanini, *J. Phys. G* **23**, 1431 (1997).
 [23] L. Corradi *et al.*, *Phys. Rev. C* **54**, 201 (1996).
 [24] C. L. Jiang, K. E. Rehm, J. Gehring, B. Glagola, W. Kutschera, M. Rhein, and A. H. Wuosmaa, *Phys. Lett. B* **337**, 59 (1994).
 [25] R. Kunkel, W. von Oertzen, H. G. Bohlen, B. Gebauer, H. A. Bosser, B. Kohlmeier, J. Speer, F. Puhlhofer, and D. Schull, *Z. Phys. A* **336**, 71 (1990).

- [26] J. Speer, W. von Oertzen, D. Schiill, M. Wilpert, H. G. Bohlen, B. Gebauer, B. Kohlmeyer, and F. Puhlhofer, *Phys. Lett. B* **259**, 422 (1991).
- [27] T. Wilpert, B. Gebauer, M. Wilpert, H. G. Bohlen, and W. von Oertzen, *Z. Phys. A* **358**, 395 (1997).
- [28] A. K. Sinha, N. Madhavan, J. J. Das, P. Sugathan, D. O. Kataria, A. P. Patro, and G. K. Mehta, *Nucl. Instrum. Methods Phys. Res. A* **339**, 543 (1994).
- [29] S. Kalkal, S. R. Abhilash, D. Kabiraj, S. Mandal, N. Madhavan, and R. Singh, *Nucl. Instrum. Methods Phys. Res. A* **613**, 190 (2010).
- [30] S. Kalkal *et al.*, *Phys. Rev. C* **81**, 044610 (2010).
- [31] L. Corradi *et al.*, *Z. Phys. A* **346**, 217 (1993).
- [32] L. Corradi *et al.*, *Z. Phys. A* **335**, 55 (1990).
- [33] S. Saha, Y. K. Agarwal, and C. V. K. Baba, *Phys. Rev. C* **49**, 2578 (1994).
- [34] L. T. Baby *et al.*, *Phys. Rev. C* **56**, 1936 (1997).
- [35] A. Winther, Computer code grazing [<http://www.to.infn.it/~nanni/grazing>].
- [36] A. Winther, *Nucl. Phys. A* **572**, 191 (1994); **594**, 203 (1995).
- [37] E. Vigezzi and A. Winther, *Ann. Phys.* **192**, 432 (1989).
- [38] L. Corradi *et al.*, *Phys. Rev. C* **66**, 024606 (2002).